

Article

Evaluation of Supercapacitive Properties of a PPY/PANI Bilayer Electrodeposited onto Carbon-Graphite Electrodes Obtained from Spent Batteries

Rafaela D. Oliveira ¹, Cleverson S. Santos ², Bruna M. Hryniwicz ³, Luís F. Marchesi ^{3,*}  and Christiana A. Pessoa ^{1,*}

¹ Departamento de Química, Universidade Estadual de Ponta Grossa (UEPG), Av. Carlos Cavalcanti, 4748, Ponta Grossa CEP 84030-900, PR, Brazil; rafa.ddoliveira@gmail.com

² Instituto Federal de Educação, Ciência e Tecnologia Farroupilha, RS-377 Km 27, Alegrete CEP 97555-000, RS, Brazil; cleversons.santos@yahoo.com.br

³ Grupo de Estudos em Espectroscopia de Impedância Eletroquímica (GEIS), Universidade Tecnológica Federal do Paraná (UTFPR), Rua Dr. Washington Subtil, 330, Ponta Grossa CEP 84017-220, PR, Brazil; brumahry@gmail.com

* Correspondence: luismarchesi@utfpr.edu.br (L.F.M.); capessoaa@uepg.br (C.A.P.)

Abstract: Recently, many efforts have been made to reuse spent batteries in response to the growing demand for sustainable materials production. In parallel, supercapacitors have attracted significant attention for their use in addressing some of the limitations of conventional capacitors and batteries. In this context, this paper describes the preparation, characterization, and supercapacitive performance evaluation of carbon-graphite (CG) electrodes obtained from spent zinc–carbon batteries and modified with polypyrrole (PPY) and polyaniline (PANI). The parameters of PPY and PANI electropolymerization were optimized. CG/PPY, CG/PANI, and CG/PPY/PANI electrodes were obtained to compare their electrochemical responses. Cyclic voltammetry (CV), galvanostatic charge–discharge curves (GCDC), and electrochemical impedance spectroscopy (EIS) were used to evaluate the pseudocapacitive properties of the CG/PPY/PANI-modified electrode. The CG/PPY/PANI electrode showed a specific capacitance of 3416 mF cm^{-2} in a current density of 2 mA cm^{-2} and a retention capacity of 76% after 850 GCDC cycles. Thus, CG/PPY/PANI electrodes are shown to be good candidates for use in the development of energy storage devices. In addition, reused CG electrodes from spent batteries have other advantages like low cost, facile construction, and environmental friendliness.

Keywords: polypyrrole; polyaniline; carbon graphite; supercapacitors



Citation: Oliveira, R.D.; Santos, C.S.; Hryniwicz, B.M.; Marchesi, L.F.; Pessoa, C.A. Evaluation of Supercapacitive Properties of a PPY/PANI Bilayer Electrodeposited onto Carbon-Graphite Electrodes Obtained from Spent Batteries. *Processes* **2024**, *12*, 31. <https://doi.org/10.3390/pr12010031>

Academic Editors: Jilei Ye, Zhuoyuan Zheng and Fausto Gallucci

Received: 25 October 2023

Revised: 11 December 2023

Accepted: 20 December 2023

Published: 22 December 2023



Copyright: © 2023 by the authors. Licensee MDPI, Basel, Switzerland. This article is an open access article distributed under the terms and conditions of the Creative Commons Attribution (CC BY) license (<https://creativecommons.org/licenses/by/4.0/>).

1. Introduction

The global demand for energy and portable electronic equipment has been increasing significantly in recent years. Currently, non-rechargeable batteries such as alkaline and zinc–carbon batteries are widely used for portable domestic household appliances due to their low cost. However, these batteries have a short useful life and need to be replaced frequently [1,2]. Efforts have been devoted to recycling spent batteries and developing efficient energy storage devices to reduce the negative environmental impact. Zinc–carbon batteries are a type of non-rechargeable battery composed of zinc coating as an anode and carbon graphite (CG) as a cathode. Lately, many methods for recycling batteries have been described in the literature, focusing on the metals present in these batteries; nonetheless, carbon rods also hold significant value for different applications. This component can be reused as an electrode for electrochemical devices. In addition, there are other advantages such as low cost, good mechanical rigidity, and environmental friendliness. Carbon-graphite electrodes are generally versatile because they can be easily modified using

different methods, which quality leads to a wide variety of electrochemical applications [3,4]. In this line, Santos et al. developed a modified electrode via electrodeposition of cobalt hydroxide onto an expanded carbon-graphite electrode (CG) obtained from spent batteries. This electrode showed a capacity of 3.4 C cm^{-2} in an applied current density of 1.0 mA cm^{-2} and a capacity retention of 91% after 1400 cycles of GCDC [5].

Another challenge lies in developing more efficient and renewable energy storage devices aimed at providing greener and more sustainable energy solutions. In this context, electrochemical storage devices have been extensively researched due to the characteristics that make them suitable for such applications. Supercapacitors (SCs) exhibit desirable characteristics, including rapid charge/discharge rates, a prolonged cycle life, and high specific power and energy densities. Furthermore, they can be constructed using environmentally friendly materials, contributing to both sustainability and cost-effectiveness [6,7]. Supercapacitors can be classified as double-layer capacitors (EDLCs), pseudocapacitors, and hybrid capacitors that have a different charge storage mechanism. In EDLCs, the charge accumulation arises at the electrode/electrolyte interface. These SCs are based on carbonaceous materials, demonstrating better cycling stability and mechanical strength [8,9]. Pseudocapacitors store energy via fast redox reactions at the electroactive material and are usually based on metals oxides/hydroxides and conducting polymers, presenting high specific capacitance but limited performance [10]. Finally, hybrid electrodes combine the properties of these two categories, providing higher specific power and energy density [11,12].

In general, conducting polymers, such as polyaniline (PANI), polythiophene (PT), poly(3,4-ethylenedioxy thiophene) (PEDOT), poly(o-phenylenediamine), and polypyrrole (PPY), are attractive materials for the development of energy storage devices due to their high conductivity, controllable thickness, cost-effectiveness, and good affinity with other materials, such as carbon-based materials [13–15]. Regarding the application of conducting polymers in energy storage devices, PANI and PPY are the most promising conducting polymers, since both have high electrical conductivity, low cost, a reversible redox rate, facile synthesis, high electron mobility, and a fast doping/dedoping rate [16]. PANI stands out due to its high theoretical specific capacitance ($\sim 2000 \text{ F g}^{-1}$), relatively easy synthesis, and superior electrochemical properties [17]. PPY, meanwhile, has a relatively high electronic conductivity (10^{-3} – 100 S cm^{-1}) in addition to easy synthesis and fast charge transfer kinetics [18].

In this regard, Budi et al. fabricated a composite polyaniline/polypyrrole-modified electrode via the electrodeposition method. The authors observed a very porous film of polyaniline and polypyrrole, while their composite formed a dense film with a relatively flat surface morphology. The electrode modified with only polyaniline presented a better charge transfer ability when compared to polyaniline and the composite; however, the electrode modified with the composite delivered a specific capacitance of 530.96 F g^{-1} [19]. Dubal et al. demonstrated a novel approach to the preparation of a layered polyaniline/polypyrrole nanocomposite using a simple oxidative chemical polymerization. The modified electrode presented an excellent electrochemical performance, including high specific capacitance (737 F g^{-1}) and a very good, stable cycle life (84% after 2000 cycles) [20]. Kandulna et al. modified an electrode with a ternary nanocomposite composed of polypyrrole/polyaniline/zinc oxide. It was observed that an aggregated nanoflake structure formed due to the formation of zinc oxide nanofillers in the surface of the polypyrrole/polyaniline composite. The GCDC showed a relatively high discharge time ($\sim 2600 \text{ s}$) and a specific capacitance of 643.75 F g^{-1} in an applied current of 0.2 A g^{-1} [16].

Given the aforementioned points, this study aims to elucidate the development of a modified electrode through the electropolymerization of polypyrrole and polyaniline on carbon-graphite electrodes obtained from spent batteries and the characterization of its electrochemical properties, particularly in terms of its supercapacitive properties.

2. Materials and Methods

All reagents were analytical grade. Aniline (ANI) (Aldrich) and pyrrole (PY) (Aldrich) were distilled under low pressure before use and stored in the refrigerator. Distilled water was used to prepare all solutions. Carbon-graphite (CG) electrodes with a geometric area of 0.126 cm^2 and a length of 4.5 cm were obtained from spent Leclanché batteries. The samples of batteries came from a collection point of spent batteries. Before use, CG electrodes were cleaned by washing them in chloroform, ethyl alcohol, and distilled water. After that, a commercial epoxy resin was used to isolate the CG active surface area. Finally, the extremities of the CG electrodes were mechanically polished using sandpaper (grit 1200 and 2000 μm).

All the electrochemical experiments were performed in an Potentiostat/Gavanostat Autolab PGSTAT 30. The CG electrodes were expanded under potentiostatic conditions by applying $+2.0 \text{ V}$ vs. $\text{Ag}/\text{AgCl}/\text{Cl}^{-\text{sat}}$ for 750 s in a 0.5 mol L^{-1} H_2SO_4 solution, as described previously in the literature [5]. Then, the electropolymerization of PY under potentiostatic conditions was performed in a 0.5 mol L^{-1} PY and 0.1 mol L^{-1} LiClO_4 solution, obtaining in this way a CG/PPY electrode at several galvanostatic charges and applied potentials. After this, the electropolymerization of PANI on the CG/PPY electrode was also carried out under potentiostatic conditions in a 0.5 mol L^{-1} ANI and 0.5 mol L^{-1} H_2SO_4 solution, producing a CG/PPY/PANI electrode while also varying the electrochemical charge and the applied potential (Figure 1).

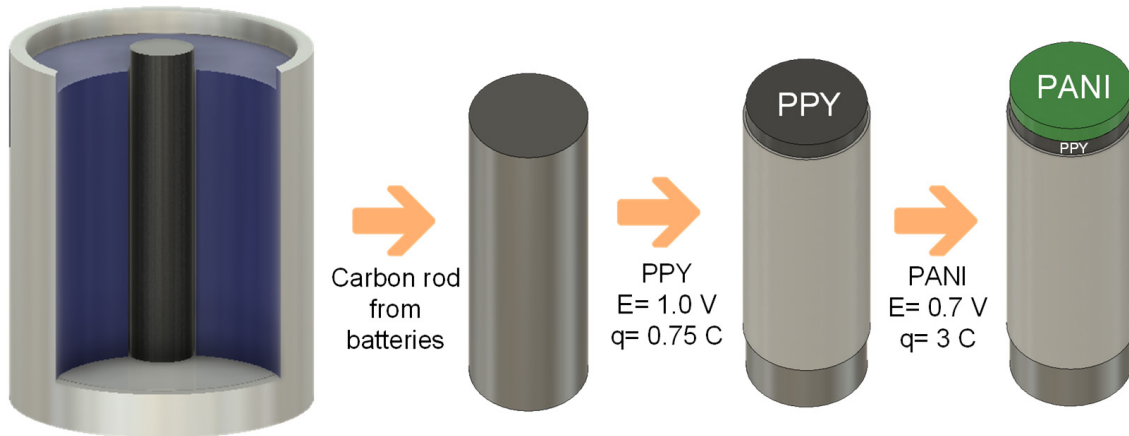


Figure 1. Representation of the synthesis of PPY and PANI onto expanded graphite electrodes from spent batteries.

The CG/PPY, CG/PANI, and CG/PPY/PANI electrodes were characterized using field emission scanning electron microscopy (FE-SEM) (TESCAN MIRA model VEGA3 operated at 15 kV combined with energy dispersive spectroscopy (EDS) and elemental mapping), Raman spectroscopy (BRUKER Senterra) and Fourier Transform Infrared spectroscopy (FTIR) (Shimadzu IR Prestige 21 spectrophotometer). Raman measurements were carried out in the range from 200 to 2500 cm^{-1} at 3.5 mW of power using a green laser with a wavelength of 532 nm. FTIR measurements were carried out in the range from 4000 to 400 cm^{-1} using a reflectance mode with 4 cm^{-1} resolution. X-ray diffraction (XRD) (Rigaku Ultima IV) measurements were performed using the radiation of $\text{Cu K}\alpha$ with a wavelength of 1.54 \AA collecting in a continuous scanning mode in a 2θ range from 10 to 80°.

A three-electrode cell configuration with the modified electrode (CG/PPY or CG/PPY/PANI) as the working electrode, a Pt wire as a counter electrode, and an $\text{Ag}/\text{AgCl}/\text{Cl}^{-\text{sat}}$ electrode as the reference was used in the electrochemical measurements. Cyclic voltammetry (CV), galvanostatic charge and discharge curves (GCDC), and electrochemical impedance spectroscopy (EIS) measurements were performed. All electrochemical characterizations were carried out in a 0.1 mol L^{-1} LiClO_4 solution. EIS was performed using open circuit potential (OCP), with an applied ac potential of 0.01 V in a frequency range from 10 kHz to 10 mHz. NOVA

2.0 software was used to control the CV, GCDC, and EIS experiments. All results shown herein are the representative ones.

3. Results and Discussion

As previously reported, the CG electrode expansion provides an increase in the electroactive surface area, which improves ionic access to the electroactive sites and the available area for charge storage [5]. In this work, we use the expanded CG electrode as a substrate for a new energy storage device based on conducting polymers. The XRD pattern of the expanded graphite is shown in Figure S1. The peaks corresponding to the (101), (004), and (110) planes of carbon graphite can be readily observed in the XRD pattern [21]. Additionally, the (002) plane of the aromatic layer exhibits a peak at 26.41° , while a small peak emerges around 42.36° related to the reflection in the (100) plane of the aromatic layer [21]. Notably, the interlayer spacing d_{002} for the expanded graphite was calculated as 0.3464 nm, slightly exceeding the standard graphite interlayer spacing of 0.3354 nm, a consequence of the expansion process [22].

Initially, the expanded CG electrode was submitted to pyrrole electropolymerization by applying +1.0 V vs. Ag/AgCl/Cl[−]_{sat} until different galvanostatic charges were achieved to obtain the CG/PPY-modified electrodes. Figure 2a shows the voltammetric behavior of a CG/PPY-modified electrode with a quasi-rectangular shape, with the presence of PPY redox peaks indicating pseudocapacitive properties. The current intensity was increased in the materials synthesized using higher galvanostatic charges until reaching the charge of 0.75 C. At higher values, it is probable that the polymeric layer is thick enough to hamper ionic intercalation during the redox process. The galvanostatic charge–discharge curves (GCDC) are in agreement with the CV results (Figure 2a), showing an increase in the discharge time with the galvanostatic charge and presenting the maximum value for the modified electrode at 0.75 C. In Figure S2 (Supporting Information), the reader can find the GCDC of the non-expanded and expanded CG electrodes.

To evaluate the GCDC as a function of the galvanostatic charge used to obtain the CG/PPY electrodes, the specific capacitance (C_{sp}) was calculated according to the following equation [23]:

$$C_{sp} = \frac{I \cdot t}{\Delta E \cdot A} \quad (1)$$

where I represents the applied current (A), t the discharge time (s), ΔE the discharge potential range (V), and A the geometrical area (cm²). In this way, the following specific capacitances were found for galvanostatic charges of 0.15, 0.30, 0.45, 0.60, 0.75, and 0.90 C: 235, 320, 374, 564, 824, and 821 mF·cm^{−2}, respectively (Figure 2b). The calculated values for non-expanded and expanded CG electrodes were 1.50 and 9.55 mF·cm^{−2}, respectively. Thus, the charge of 0.75 C was chosen as the optimum value to obtain the CG/PPY-modified electrode. Furthermore, the applied potential for the electrochemical synthesis of PPY was studied in the range of +0.8 to +1.2 V. According to the literature, pyrrole electropolymerization can be carried out at different potential values. The CV curves for CG/PPY obtained at different potentials showed similar intensities of current (Figure 2c), indicating that the electrodes had almost the same amount of electroactive material. As shown in Figure 2d, the GCDC exhibited similar charge–discharge times for the +1.0 and +1.2 V applied potentials, with respective C_{sp} values of 824 and 804 mF cm^{−2}. Therefore, the CG/PPY-modified electrode obtained using an applied potential of +1.0 V and a galvanostatic charge of 0.75 C was chosen to proceed with the experiments.

The next step was to study PANI electropolymerization on CG/PPY to obtain the CG/PPY/PANI-modified electrodes. Figure 3a shows that the CV response of PANI, synthesized using electropolymerization at an applied potential of +0.7 V to produce CG/PPY/PANI-modified electrodes, exhibited an increment in the current intensity until reaching the galvanostatic charge of 3 C. However, the GCDC showed a higher discharge time for the CG/PPY/PANI electrode with PANI electropolymerized using a galvanostatic charge of 3 C (Figure 3b). The C_{sp} values calculated were 1417, 1992, 2886, and

2838 mF cm⁻² for 1, 2, 3, and 3.25 C, respectively. Considering these results, the galvanostatic charge of 3 C was chosen for the electropolymerization of PANI based on the GCDC response of the CG/PPY/PANI-modified electrode.

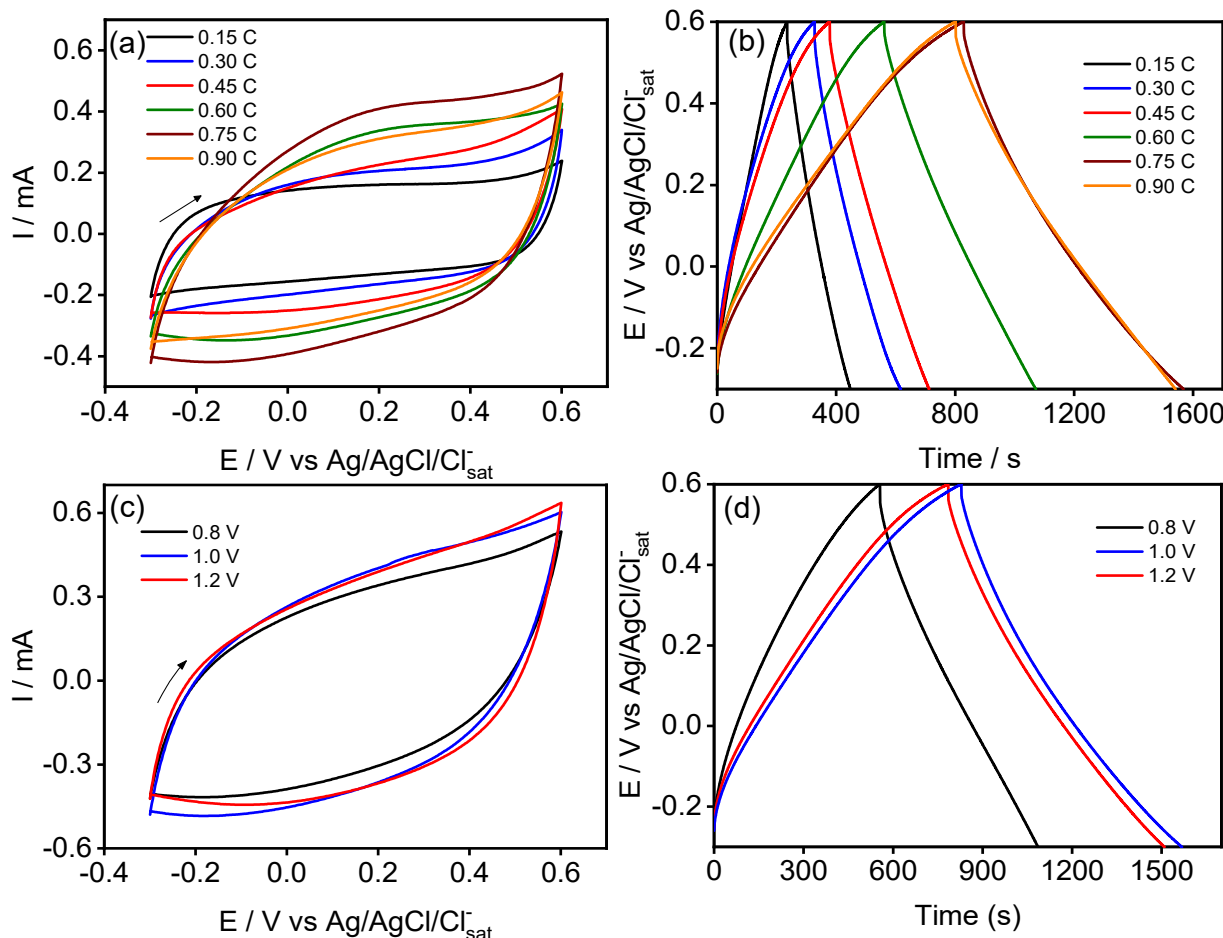


Figure 2. (a) CV and (b) GCDC for CG/PPY-modified electrodes obtained via electropolymerization at +1.0 V and different galvanostatic charge values; (c) CV and (d) GCDC for CG/PPY-modified electrodes obtained via electropolymerization with $q = 750$ mC and different applied potentials. Supporting electrolyte: 0.1 mol L⁻¹ LiClO₄. RE: Ag/AgCl/Cl⁻_{sat}. CE: Platinia. Scan rate of 5 mV s⁻¹. $j = 1$ mA cm⁻².

The applied potential for PANI electrochemical synthesis was studied in the range of +0.7 to +0.9 V. The CVs obtained for CG/PPY/PANI are shown in Figure 3c. Similar current intensities can be observed for PANI electropolymerized at these potentials. Nevertheless, the GCDC (Figure 3d) showed different charge–discharge times. C_{sp} values of 2886, 3416, and 2459 mF cm⁻² were obtained for CG/PPY/PANI, with PANI electrochemically synthesized at applied potentials of 0.7, 0.8, and 0.9 V, respectively. The CG/PPY/PANI-modified electrode presents better GCDC performance when obtained at +0.8 V. Thus, based on these results, the optimized conditions to obtain CG/PPY/PANI-modified electrodes were determined as follows: $E = +1.0$ V and $q = 0.75$ C for PPY, and $E = 0.8$ V and $q = 3.0$ C for PANI electropolymerization.

To evaluate the electrochemical performance of the modified electrode, the electrochemical behaviors of CG/PPY, CG/PANI, and CG/PPY/PANI were compared. The CV results shown in Figure 4a highlight a notably higher current for CG/PPY/PANI compared to CG/PPY and similar current intensities between the CG/PANI and CG/PPY/PANI electrodes. However, the GCDC results evidence a higher discharge time for the CG/PPY/PANI-modified electrode when compared to the other electrodes (Figure 4b). This leads to an

increment in the C_{sp} values, which were calculated as 613, 1216, and 1417 mF cm^{-2} for the CG/PPY-, CG/PANI-, and CG/PPY/PANI-modified electrodes, respectively, as presented in Figure 4c. Considering the behavior present in the CV (a quasi-rectangular profile) and the GCDC (a quasi-triangular profile) responses of the modified electrodes, it can be assumed that the redox reactions are occurring at the surface of the electrode followed by an intercalation process [24]. The enhancement of the supercapacitive properties in the presence of PANI highlights the potential for using the combination of both polymers in the construction of an energy storage device.

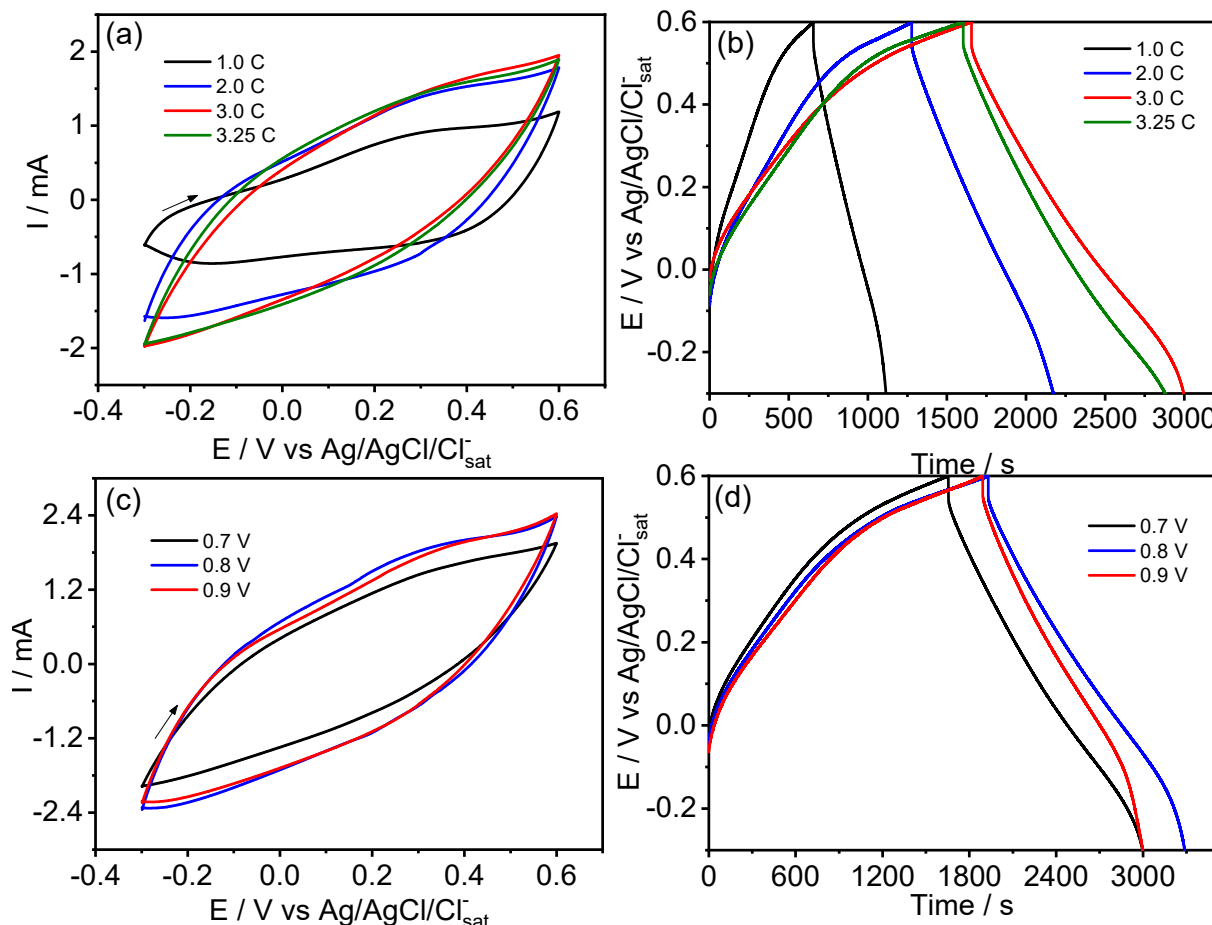


Figure 3. (a) CV and (b) GCDC for CG/PPY/PANI-modified electrodes obtained via electropolymerization at +0.7 V and at different galvanostatic charge values; (c) CV and (d) GCDC for CG/PPY/PANI-modified electrodes obtained via electropolymerization with $q = 3 \text{ C}$ and different applied potentials. Supporting electrolyte: $0.1 \text{ mol L}^{-1} \text{ LiClO}_4$. RE: Ag/AgCl/Cl[−]_{sat}. CE: Platina. Scan rate of 5 mV s^{-1} . $j = 2 \text{ mA cm}^{-2}$.

The material morphologies were evaluated via field emission scanning electron microscopy (FE-SEM), as can be seen in Figure 5. All the samples showed a similar globular morphology characteristic of conducting polymers [25]. The surface of the CG/PANI electrode (Figure 5a) shows more heterogeneity than the CG/PPY electrode, with an evident number of globular structures (Figure 5b). The SEM image of the CG/PPY/PANI electrode (Figure 5c) also shows agglomerated globules at the surface, indicating the presence of PANI.

Figure 6 shows the FTIR spectra obtained for the CG/PPY-, CG/PANI-, and CG/PPY/PANI-modified electrodes. In the CG/PPY spectra, the vibration of the pyrrole ring was observed at 1595 cm^{-1} and the C–N stretching appeared at 1256 cm^{-1} . The bands at 1003 and 868 cm^{-1} were attributed to out-of-plane C–H bending vibrations [26]. The CG/PANI spectra also

revealed $=\text{C}-\text{H}$ in-plane deformation at 1371 cm^{-1} and $=\text{C}-\text{H}$ out-of-plane vibrations at 962 and 854 cm^{-1} . The band related to $\text{C}-\text{N}$ stretching vibration appeared at 1204 cm^{-1} [27]. The FTIR spectrum of CG/PPY/PANI presented all the prominent features of PPY and PANI, revealing the existence of both polymers in the modified electrode. The bands at 1516 and 1210 cm^{-1} were ascribed to the vibration of the pyrrole ring and $\text{C}-\text{N}$ stretching, respectively. The in-plane $=\text{C}-\text{H}$ bending was observed at 1367 cm^{-1} and out-of-plane $=\text{C}-\text{H}$ vibrations appeared at 860 and 903 cm^{-1} .

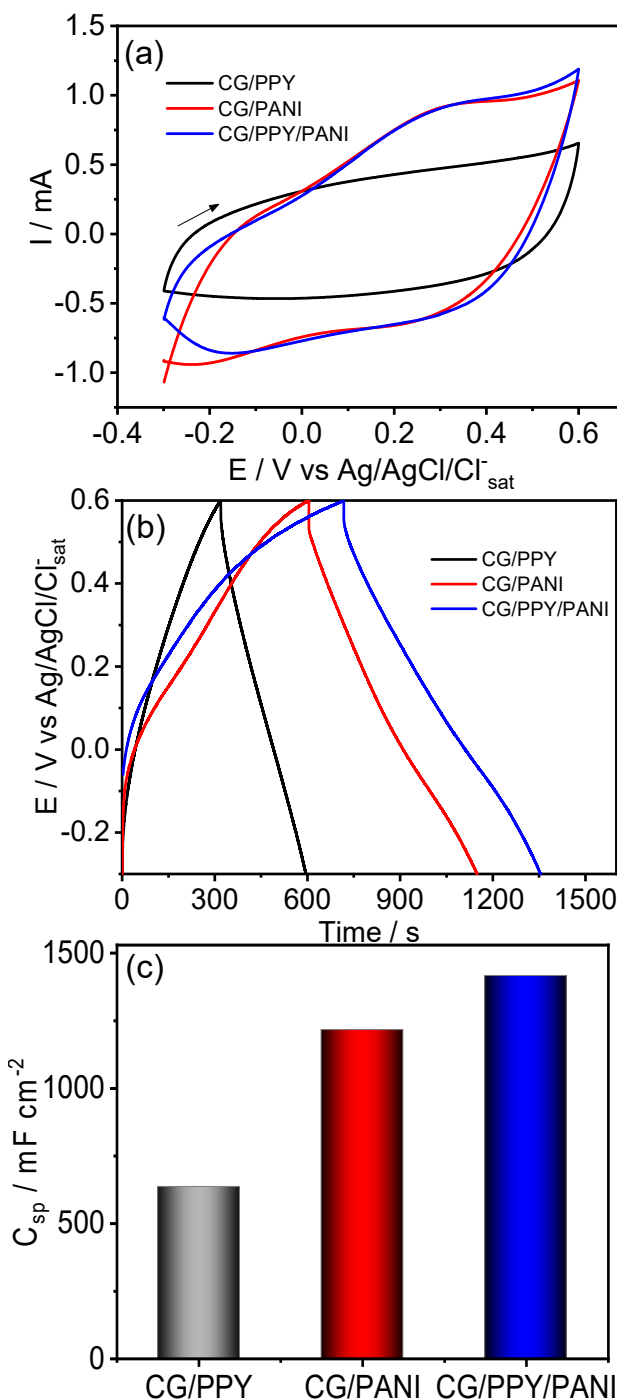


Figure 4. (a) CV, (b) GCDC, and (c) C_{sp} for CG/PPY-, CG/PANI-, and CG/PPY/PANI-modified electrodes. Supporting electrolyte: $0.1\text{ mol L}^{-1}\text{ LiClO}_4$. RE: Ag/AgCl/Cl⁻_{sat}. CE: Platina. Scan rate of 5 mV s^{-1} . $j = 2\text{ mA cm}^{-2}$.

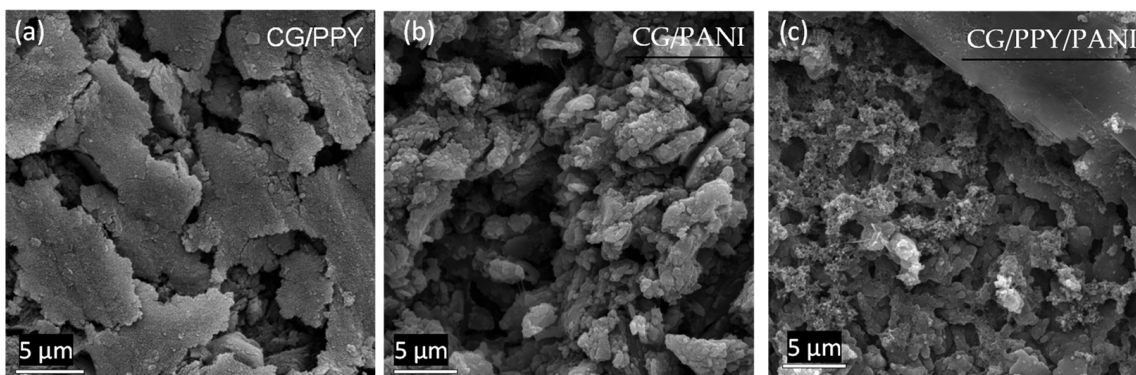


Figure 5. Representative FE-SEM images from (a) CG/PPY, (b) CG/PANI, and (c) CG/PPY/PANI electrodes.

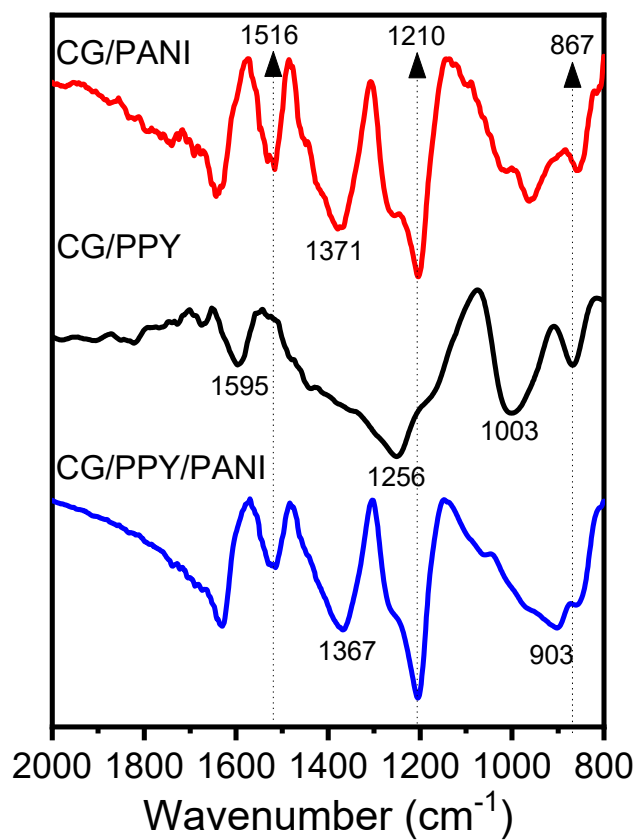


Figure 6. FTIR spectra from the CG/PPY-, CG/PANI-, and CG/PPY/PANI-modified electrodes.

In Figure 7a, Raman spectra of CG/PPY, CG/PANI, and CG/PPY/PANI are shown. The characteristic carbonaceous D and G bands are observed at 1338 and 1607 cm^{-1} , respectively, in the CG/PANI and CG/PPY/PANI spectra. In the CG/PPY electrode spectra, the D band appears at 1350 cm^{-1} and the G band at 1573 cm^{-1} . The intensity ratios (I_D/I_G) for CG/PPY, CG/PANI, and CG/PPY/PANI were calculated as 1.04 , 0.98 , and 1.15 . These values reflect the relative disorder in carbonaceous structures. The increased intensities for the CG/PPY/PANI electrode suggest a higher disorder in this material [5]. The Raman spectra of CG/PANI and CG/PPY/PANI show the band attributed to C=N quinoid structures at 1497 and 1503 cm^{-1} , respectively. This suggests a conductive, polaronic structure of PANI [28]. An out-of-plane C-H deformation of quinoid form was observed at 923 cm^{-1} for CG/PPY and a benzoid ring vibration at 967 cm^{-1} [29]. The C-H bending of the PANI benzoid structure was observed at 1170 cm^{-1} for CG/PANI and CG/PPY/PANI [30].

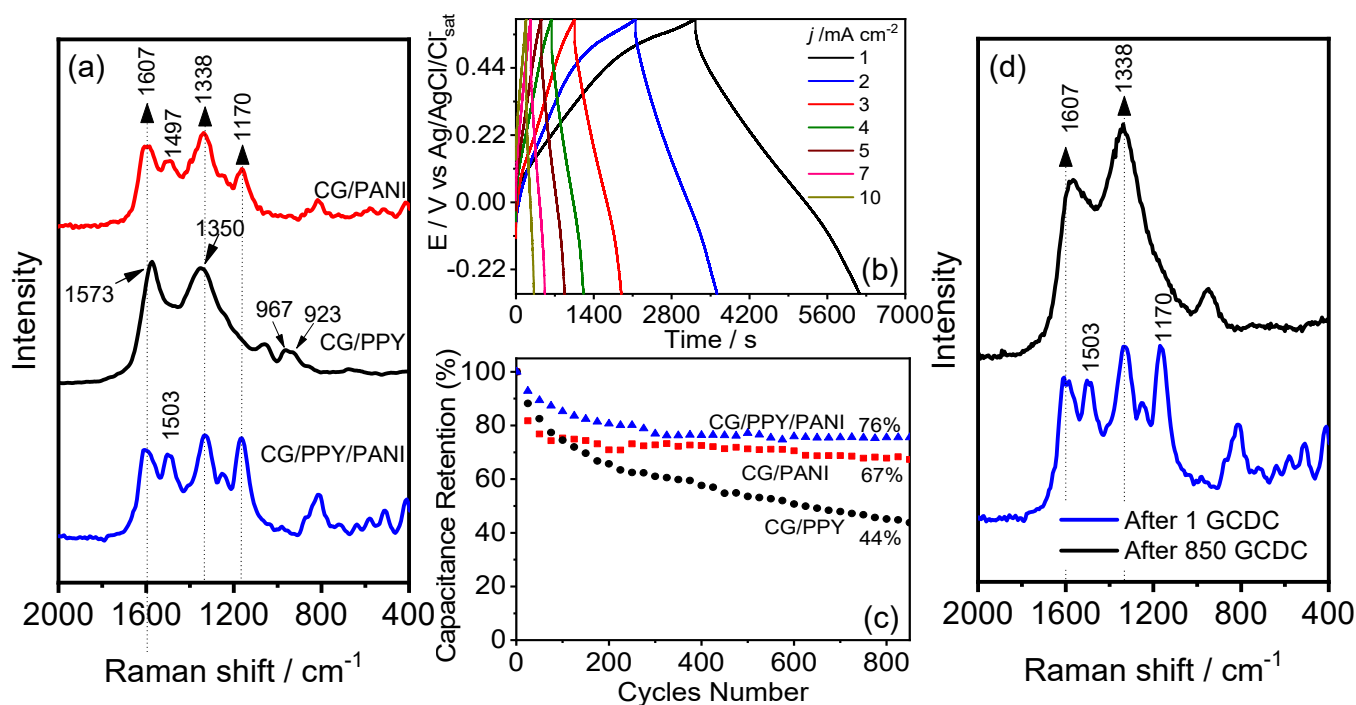


Figure 7. (a) Raman spectra for the CG/PPY, CG/PANI, and CG/PPY/PANI electrodes; (b) the GCDC of the CG/PPY/PANI-modified electrodes at different current densities; (c) the capacitance retention of the CG/PPY, CG/PANI, and CG/PPY/PANI electrodes; (d) Raman spectra for the CG/PPY/PANI electrode after 1 cycle and 850 cycles of GCDC.

Electrochemical characterization of the CG/PPY/PANI electrode was carried out using GCDC and EIS measurements. Figure 7b shows the GCDC performance at different current densities for the CG/PPY/PANI-modified electrode. One can observe a decrease in the discharge time with the current density. This behavior occurs because, in high current densities, there is not enough time for the ions to intercalate into the polymeric matrix to reach an active site, resulting in a lower charge accumulation, which is reflected in the discharge time [31]. The following C_{sp} values were calculated using Equation 1 and are presented in Table 1.

Table 1. Specific capacitances obtained for CG/PPY/PANI electrode at different current densities.

| Current Density/mA cm ⁻² | Specific Capacitance/mF cm ⁻² |
|-------------------------------------|--|
| 1 | 3431 |
| 2 | 3416 |
| 3 | 2998 |
| 4 | 2792 |
| 5 | 2608 |
| 7 | 2320 |
| 10 | 1968 |

The capacitance retention was evaluated for CG/PPY, CG/PANI, and CG/PPY/PANI electrodes across 850 GCDC cycles at a current density of 10 mA cm⁻² (Figure 7c). The CG/PPY revealed lower retention capacitance, which gradually declined to 44% of initial C_{sp} . The CG/PANI and CG/PPY/PANI electrodes showed similar capacitance retention curves, with a sharp decrease over 200 cycles followed by an almost constant value, resulting in C_{sp} values of 67% and 76%, respectively. As studied by Hryniwicz et al., the decline in the specific capacitance of pseudocapacitive materials derived from PPY is attributed to morphological changes during GCDC. This is a result of the swelling and shrinkage of the polymeric matrix induced by consecutive oxidation and reduction processes [32].

This effect leads to an increase in the charge transfer resistance (R_{ct}), also observed in other works [33,34]. The heightened R_{ct} contributes to ineffective electrolyte ion diffusion within the polymeric matrix during the redox process and consequently leads to a reduction in specific capacitance. However, when PANI is present, this initial decline in capacitance is less abrupt, consistent with findings from other studies [35].

Figure 7d presents the Raman spectrum of the CG/PPY/PANI electrode before and after the cycling experiment. A shift in the G band was observed from 1607 cm^{-1} (as-synthesized materials) to 1567 cm^{-1} (after the capacitance retention study). However, the D band did not shift after the experiment, remaining at 1338 cm^{-1} . The intensity ratio (I_D/I_G) changed from 1.15 to 1.22 after the cycling process. These results might suggest an exposure of the CG electrode during the cycles and an increase in the disorder of the carbonaceous structures [36]. Furthermore, the disappearance of the band at 1170 cm^{-1} (attributed to the C-H bending of benzoind PANI) and the appearance of a band at approximately 948 cm^{-1} —potentially arising from an overlap between the PPY bands at 967 cm^{-1} and 923 cm^{-1} —in the post-cycling spectrum suggest a morphological degradation of the PANI film, promoting a better exposure of the PPY structure.

The FE-SEM images of the CG/PPY/PANI electrode before and after 850 GCDC cycles are shown in Figure 8. Changes in the material surface can be observed after the cycling experiment, mainly in the morphology homogeneity. This behavior was observed before for PPY nanotubes synthesized in stainless steel mesh electrodes and might be the reason for the capacitance loss during the cycles [32]. Herein, the appearance of pores at the electrode surface and the formation of agglomerated globular structures can be observed. Figure 8b shows globular structures characteristic of conducting polymers, indicating that PANI and PPY remain at the electrode surface after 850 cycles but with slightly different morphologies.

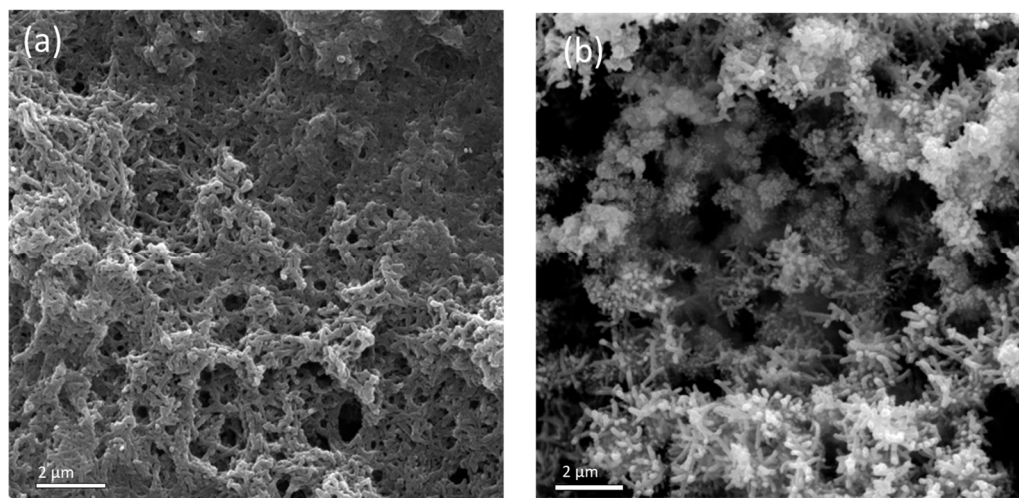


Figure 8. Representative FE-SEM images from (a) CG/PPY/PANI electrode before and (b) CG/PPY/PANI electrode after 850 consecutive cycles.

Table 2 shows the response of the modified electrode developed in this work in contrast to different electrodes found in the literature, including C_{sp} and retention capacitance. The CG/PPY/PANI electrode developed in this work has a comparable capacitance retention with electrodes previously described in the literature; however, it is difficult to compare the specific capacitances due to differences in normalization. Here, the capacitance values were normalized using the geometric area to obtain the C_{sp} values.

The findings of this work suggest that the utilization of expanded graphite derived from spent batteries, when modified with PPY and PANI, holds significant promise for application in supercapacitors. This not only contributes to the development of new environmentally friendly devices but also presents an opportunity for the production of

high-performance energy delivery systems, offering high specific capacitances and long cycle life.

Table 2. Performance comparison of some modified electrodes reported in the literature.

| Electrodes | C_{sp} | j | Retention Capacitance | Reference |
|--|--------------------------|-------------------------|-----------------------|-----------|
| CG/PPY/PANI | 3416 mF cm^{-2} | 2.0 mA cm^{-2} | 76% (850 cycles) | This work |
| PAn-PPy-Grt-Sp ^a | 55.4 mF cm^{-2} | 0.3 mA cm^{-2} | 80% (3000 cycles) | [37] |
| PPy@PANI/NHGR film electrode | 1348 mF cm^{-2} | 1.0 mA cm^{-2} | 73.7% (7000 cycles) | [38] |
| PANI-PPY/PET fabric conductive composite | 1046 mF cm^{-2} | 2.0 mA cm^{-2} | 54.2% (1000 cycles) | [39] |
| PANI-PPY | 723 F g^{-1} | 5.0 mA cm^{-2} | 84% (2000 cycles) | [20] |
| PPY/PANI | 348 F g^{-1} | 1.0 A g^{-1} | 51.6% (100 cycles) | [27] |
| PPY/PANI/TiN ^b | 288.4 F g^{-1} | 1.0 A g^{-1} | 78% (200 cycles) | [40] |
| PPY-PANI-ZnO | 436.14 F g^{-1} | 0.2 A g^{-1} | 90.3% (2000 cycles) | [16] |

^a PAn-PPy-Grt-Sp—Polyaniline assembled on a polypyrrole layer and deposited on graphite pencil traces in sandpaper. ^b TiN—titanium nitride.

4. Conclusions

In this work, a CG/PPY/PANI-modified electrode was constructed using a CG electrode from spent, cylindrical zinc–carbon batteries. The parameters for electrode modification were optimized by evaluating their pseudocapacitive properties, and the best performance was obtained for the CG modified with PPY and PANI synthesized under potentiostatic conditions by applying 1.0 V until reaching the electropolymerized charge of 0.75 C for PPY and 0.8 V and 3.0 C for PANI electropolymerization. The CG/PPY/PANI electrode showed a C_{sp} of 3416 mF cm^{-2} ($j = 2 \text{ mA cm}^{-2}$), and it was properly characterized using scanning electron microscopy, FTIR, and Raman spectroscopy techniques. Raman and FTIR measurements of the optimized electrode showed the main bands of PPY and PANI, indicating the presence of both conducting polymers at the electrode surface. Moreover, galvanostatic charge–discharge curves showed that the CG/PPY/PANI electrode maintained 76% of the initial C_{sp} after 850 cycles, which is higher than the capacitance retention obtained for the CG/PPY and CG/PANI electrodes. Raman and FE-SEM measurements of the modified electrode after 850 charge–discharge cycles demonstrated some surface modifications; however, the images confirmed that the conducting polymers remained at the electrode surface. Overall, the results demonstrate the fabrication of a material based on PPY and PANI with high specific capacitance and good capacitance retention, unveiling the potential of using spent batteries for the construction of environmentally friendly energy storage devices.

Supplementary Materials: The following supporting information can be downloaded at: <https://www.mdpi.com/article/10.3390/pr12010031/s1>, Figure S1: XRD pattern of carbon graphite electrode. Figure S2: GCDC of a non-expanded (black line) and expanded (red line) carbon-graphite (CG) electrode. Applied current of 1.0 mA cm^{-2} and supporting electrolyte of LiClO_4 0.1 mol L^{-1} .

Author Contributions: Conceptualization, B.M.H.; funding acquisition, L.F.M. and C.A.P.; methodology, R.D.O. and C.S.S.; formal analysis, B.M.H. and L.F.M.; writing—original draft, R.D.O. and C.S.S.; supervision, L.F.M. and C.A.P.; project administration, C.A.P. and L.F.M. All authors have read and agreed to the published version of the manuscript.

Funding: The authors would like to extend our appreciation to Universidade Tecnológica Federal do Paraná (UTFPR) for funding this work through the Edital 07/2020—PROPPG, Fundação Araucária and Conselho Nacional de Desenvolvimento Científico e Tecnológico (CNPq).

Data Availability Statement: The data presented in this study are available on request from the corresponding author.

Acknowledgments: The authors gratefully acknowledge Jarem R. Garcia from Universidade Estadual de Ponta Grossa (UEPG) for the XRD experiments.

Conflicts of Interest: The authors declare no conflict of interest.

References

1. Vadivel, S.; Tejangkura, W.; Sawangphruk, M. Graphite/Graphene Composites from the Recovered Spent Zn/Carbon Primary Cell for the High-Performance Anode of Lithium-Ion Batteries. *ACS Omega* **2020**, *5*, 15240–15246. [\[CrossRef\]](#) [\[PubMed\]](#)
2. Yoshimura, A.; Hemmi, K.; Moriwaki, H.; Sakakibara, R.; Kimura, H.; Aso, Y.; Kinoshita, N.; Suizu, R.; Shirahata, T.; Yao, M.; et al. Improvement in Cycle Life of Organic Lithium-Ion Batteries by In-Cell Polymerization of Tetrathiafulvalene-Based Electrode Materials. *ACS Appl. Mater. Interfaces* **2022**, *14*, 35978–35984. [\[CrossRef\]](#) [\[PubMed\]](#)
3. Almeida, R.H.D.; Monroy-Guzmán, F.; Juárez, C.R.A.; Rocha, J.M.; Bustos, E.B. Electrochemical detector based on a modified graphite electrode with phthalocyanine for the elemental analysis of actinides. *Chemosphere* **2021**, *276*, 130114. [\[CrossRef\]](#) [\[PubMed\]](#)
4. Ferdowsi, G.S.; Seyedsadjadi, S.A.; Ghaffarinejad, A. Ni nanoparticle modified graphite electrode for methanol electrocatalytic oxidation in alkaline media. *J. Nanostruct. Chem.* **2014**, *5*, 17–23. [\[CrossRef\]](#)
5. Santos, C.S.; Oliveira, R.D.; Marchesi, L.F.; Pessoa, C.A. Electrodeposited cobalt hydroxide in expanded carbon graphite electrode obtained from exhausted batteries applied as energy storage device. *Arab. J. Chem.* **2020**, *13*, 3448–3459. [\[CrossRef\]](#)
6. Hryniwicz, B.M.; Bach-Toledo, L.; Vidotti, M. Harnessing energy from micropollutants electrocatalysis in a high-performance supercapacitor based on PEDOT nanotubes. *Appl. Mater. Today* **2020**, *18*, 100538. [\[CrossRef\]](#)
7. Gilshtein, E.; Flox, C.; Ali, F.S.M.; Mehrabimatin, B.; Fedorov, F.S.; Lin, S.; Zhao, X.; Nasibulin, A.G.; Kallio, T. Superior environmentally friendly stretchable superior based on nitrogen-doped graphene/fydrogel and single-walled carbon nanotubes. *J. Energy Storage* **2020**, *30*, 101505. [\[CrossRef\]](#)
8. Pereira, G.F.L.; Fileti, E.E.; Siqueira, L.J.A. Comparing Graphite and Graphene Oxide Supercapacitors with a Constant Potential Model. *J. Phys. Chem. C* **2021**, *125*, 2318–2326. [\[CrossRef\]](#)
9. Chen, X.; Paul, R.; Dai, L. Carbon-based supercapacitors for efficient energy storage. *Natl. Sci. Rev.* **2017**, *4*, 453–489. [\[CrossRef\]](#)
10. Bertana, V.; Scordo, G.; Camili, E.; Ge, L.; Zaccagnini, P.; Lamberti, A.; Marasso, S.L.; Scaltrito, L. 3D Printed Supercapacitor Exploiting PEDOT-Based Resin and Polymer Gel Electrolyte. *Polymers* **2023**, *15*, 2657. [\[CrossRef\]](#)
11. Jadhav, S.A.; Dhas, S.D.; Pail, K.T.; Moholkar, A.V.; Patil, P.S. Polyaniline (PANI)-manganese dioxide (MnO_2) nanocomposites as efficient electrode materials for supercapacitors. *Chem. Phys. Lett.* **2021**, *778*, 138764. [\[CrossRef\]](#)
12. Cai, X.; Sun, K.; Qiu, Y.; Jiao, X. Recent Advances in Graphene and Conducting Polymer Composites for Supercapacitors Electrodes: A Review. *Crystals* **2021**, *11*, 947. [\[CrossRef\]](#)
13. Zhu, H.; Wang, X.; Yang, X. Integrated Synthesis of Poly(o-phenylenediamine)-Derived Carbon Materials for High Performance Supercapacitors. *Adv. Mater.* **2012**, *24*, 6524–6529. [\[CrossRef\]](#) [\[PubMed\]](#)
14. Wang, W.; Cao, J.; Yu, J.; Tian, F.; Luo, X.; Hao, Y.; Huang, J.; Wang, F.; Zhou, W.; Xu, J.; et al. Flexible Supercapacitors Based on Stretchable Conducting Polymer Electrodes. *Polymers* **2023**, *15*, 1856. [\[CrossRef\]](#) [\[PubMed\]](#)
15. Strakhov, I.S.; Rodnaya, A.I.; Mezhuev, Y.O.; Korshak, Y.V.; Vagramyan, T.A. Enhancement of the strength of a composite material based on ED-20 epoxy resin by reinforcement with a carbon fiber modified by electrochemical deposition of poly(o-phenylenediamine). *Russ. J. Appl. Chem.* **2014**, *87*, 1918–1922. [\[CrossRef\]](#)
16. Kandulna, K.; Choudhary, R.B.; Singh, R. Free Exciton Absorptions and Quasi-reversible Redox Actions in Polypyrrole-Polyaniline-Zinc Oxide Nanocomposites as Electron Transporting Layer for Organic Light Emitting Diode and Electrode Material for Supercapacitors. *J. Inorg. Organomet. Polym. Mater.* **2019**, *29*, 730–744. [\[CrossRef\]](#)
17. Wang, Q.; Li, J.; Wang, D.; Niu, J.; Du, P.; Liu, J.; Liu, P. Enhanced electrochemical performance of polyaniline-based electrode for supercapacitors in mixed aqueous electrolyte. *Electrochim. Acta* **2020**, *349*, 136348. [\[CrossRef\]](#)
18. Shi, Y.; Peng, L.; Ding, Y.; Zhao, Y.; Yu, G. Nanostructured conductive polymers for advanced energy storage. *Chem. Soc. Rev.* **2015**, *44*, 6684–6696. [\[CrossRef\]](#)
19. Budi, S.; Deswara, R.D.; Mahmud, A.; Paristiowati, M.; Handoko, E.; Sugihartono, I.; Fahdiran, R. Specific capacitance and impedance of electrodeposited polyaniline, polypyrrole and polyaniline/polypyrrole composites films. *J. Phys. Conf. Ser.* **2019**, *1402*, 066015. [\[CrossRef\]](#)
20. Dubal, D.P.; Patil, S.V.; Gund, G.S.; Lokhande, C.D. Polyaniline-polypyrrole nanograin composite via electrostatic adsorption for high performance electrochemical supercapacitors. *J. Alloys Compd.* **2013**, *552*, 240–247. [\[CrossRef\]](#)
21. Qiu, T.; Yang, J.G.; Bai, X.J.; Wang, Y.L. The preparation of synthetic graphite materials with hierarchical pores from lignite by one-step impregnation and their characterization as dye absorbents. *RSC Adv.* **2019**, *9*, 12737–12746. [\[CrossRef\]](#) [\[PubMed\]](#)
22. Zhao, T.; She, S.; Ji, X.; Guo, X.; Jin, W.; Zhu, R.; Dang, A.; Li, H.; Li, T.; Wei, B. Expanded graphite embedded with aluminum nanoparticles as superior thermal conductivity anodes for high-performance lithium-ion batteries. *Sci. Rep.* **2016**, *6*, 33833. [\[CrossRef\]](#) [\[PubMed\]](#)
23. Liu, W.; Yan, X.; Chen, J.; Feng, Y.; Xue, Q. Novel and high-performance asymmetric micro-supercapacitors based on graphene quantum dots and polyaniline nanofibers. *Nanoscale* **2013**, *5*, 6053–6062. [\[CrossRef\]](#) [\[PubMed\]](#)
24. Fleischmann, S.; Mitchell, J.B.; Wang, R.; Zhan, C.; Jiang, D.-E.; Presser, V.; Augustyn, V. Pseudocapacitance: From Fundamental Understanding to High Power Energy Storage Materials. *Chem. Rev.* **2020**, *120*, 6738–6782. [\[CrossRef\]](#) [\[PubMed\]](#)
25. Hao, L.; Dong, C.; Zhang, L.; Zhu, K.; Yu, D. Polypyrrole Nanomaterials: Structure, Preparation and Application. *Polymers* **2022**, *14*, 5139. [\[CrossRef\]](#) [\[PubMed\]](#)

26. Liang, B.; Qin, Z.; Li, T.; Dou, Z.; Zeng, F.; Cai, Y.; Zhu, M.; Zhou, Z. Poly(aniline-co-pyrrole) on the surface of reduced graphene oxide as high-performance electrode materials for supercapacitors. *Electrochim. Acta* **2015**, *177*, 335–342. [\[CrossRef\]](#)

27. Lei, W.; He, P.; Zhang, S.; Dong, F.; Ma, Y. One-step triple-phase interfacial synthesis of polyaniline-coated polypyrrole composite and its application as electrode materials for supercapacitors. *J. Power Sources* **2014**, *266*, 347–352. [\[CrossRef\]](#)

28. Marchesi, L.M.; Jacumasso, S.C.; Quintanilha, R.C.; Winnischofer, H.; Vidotti, M. The electrochemical impedance spectroscopy behavior of poly(aniline) nanocomposite electrodes modified by Layer-by-Layer deposition. *Electrochim. Acta* **2015**, *174*, 864–870. [\[CrossRef\]](#)

29. Santos, M.J.L.; Brolo, A.G.; Girotto, E.M. Study of polaron and bipolaron states in polypyrrole by in situ Raman spectroelectrochemistry. *Electrochim. Acta* **2007**, *52*, 6141–6145. [\[CrossRef\]](#)

30. Deshmukh, S.P.; Dhodamani, A.G.; Patil, S.M.; Mullani, S.B.; More, K.V.; Deleka, S.D. Interfacially interactive ternary silver-supported polyaniline/multiwalled carbon nanotube nanocomposites for catalytic and antibacterial activity. *ACS Omega* **2020**, *5*, 219–227. [\[CrossRef\]](#)

31. Dupont, M.F.; Donne, S.W. Charge storage mechanisms in electrochemical capacitors: Effects of electrode properties on performance. *J. Power Sources* **2016**, *326*, 613–623. [\[CrossRef\]](#)

32. Hryniwicz, B.M.; Lima, R.V.; Marchesi, L.F.; Vidotti, M. Impedimetric studies about the degradation of polypyrrole nanotubes during galvanostatic charge and discharge cycles. *J. Electroanal. Chem.* **2019**, *855*, 113636. [\[CrossRef\]](#)

33. Huang, Y.; Zhu, M.; Pei, Z.; Huang, Y.; Geng, H.; Zhi, C. Extremely Stable Polypyrrole Achieved via Molecular Ordering for Highly Flexible Supercapacitors. *Electrochim. Acta* **2016**, *8*, 2435–2440. [\[CrossRef\]](#) [\[PubMed\]](#)

34. Hamra, A.A.B.; Lim, H.N.; Hafiz, S.M.; Kamaruzaman, S.; Abdul Rashid, S.; Yunus, R.; Altarawneh, M.; Jiang, Z.T.; Huang, N.M. Performance stability of solid-state polypyrrole-reduced graphene oxide-modified carbon bundle fiber for supercapacitor application. *Electrochim. Acta* **2018**, *285*, 9–15. [\[CrossRef\]](#)

35. Liu, T.; Finn, L.; Yu, M.; Wang, H.; Zhai, T.; Lu, X.; Tong, Y.; Li, Y. Polyaniline and Polypyrrole Pseudocapacitor Electrodes with Excellent Cycling Stability. *Nano Lett.* **2014**, *14*, 2522–2527. [\[CrossRef\]](#) [\[PubMed\]](#)

36. Wan, C.; Jiao, Y.; Li, J. Flexible, highly conductive, and free-standing reduced graphene oxide/polypyrrole/cellulose hybrid papers for supercapacitor electrodes. *J. Mater. Chem. A* **2017**, *5*, 3819–3831. [\[CrossRef\]](#)

37. Alcaraz-Espinoza, J.J.; Oliveira, H.P. Flexible supercapacitor based on a ternary composite of polyaniline/polypyrrole/graphite on gold coated sandpaper. *Electrochim. Acta* **2018**, *274*, 200–207. [\[CrossRef\]](#)

38. Zhang, G.; Zhang, J.; Li, W.; Wang, J.; Li, X. Flexible core/shelled Ppy@PANI nanotube porous films for hybrid supercapacitors. *Nanotechnology* **2022**, *33*, 065407. [\[CrossRef\]](#) [\[PubMed\]](#)

39. Xie, X.; Xin, B.; Chen, Z.; Xu, Y. Preparation and characterization of PANI-PPY/PET fabric conductive composite for supercapacitors. *J. Text. Inst.* **2022**, *113*, 2443–2450. [\[CrossRef\]](#)

40. Xie, Y.; Wang, D. Supercapacitance performance of polypyrrole/titanium nitride/polyaniline coaxial nanotube hybrid. *J. Alloys Compd.* **2016**, *665*, 323–332. [\[CrossRef\]](#)

Disclaimer/Publisher's Note: The statements, opinions and data contained in all publications are solely those of the individual author(s) and contributor(s) and not of MDPI and/or the editor(s). MDPI and/or the editor(s) disclaim responsibility for any injury to people or property resulting from any ideas, methods, instructions or products referred to in the content.